Jour. Korean Earth Science Society, v. 30, no. 1, p. 69–80, February 2009

Star Formation Rate and AGN in Barred Galaxies

Bang Jun[1] and Hong Bae Ann[2,*]

[1]Korea Science Academy, Busan 614-822, Korea
[2]Division of Science Education, Pusan National University, Busan 609-735, Korea

막대은하의 별탄생율과 활동성 은하핵

방 준[1] · 안홍배[2,*]

[1]한국과학영재학교, 614-822, 부산시 부산진구 당감3동 899
[2]부산대학교 과학교육학부, 635-749, 부산시 금정구 장전동 산30

Abstract: We investigate the dependence of star formation rate and Active Galaxy Nuclei (AGN) frequency on the bar properties, especially the bar strength, using SDSS DR6. To better represent the bar strength, we divided the bars into 6 classes according to their length and axial ratios. There seems to be a fairly good correlation between the star formation rate derived from Hα emission lines and the bar strength, whereas there is no apparent correlation between the AGN activity and the bar strength. We interpret that the former correlation is due to the dependence of bar-driven gas inflow on the strength of bar. The lack of correlation between AGN and bar properties suggests that the accretion of gas onto a supermassive black hole (SMBH) is regulated by the interplay between the bar and SMBH. The frequency of AGN seems to be dependent on the background density but the star formation rate does not. It suggests that star formation is a localized phenomenon that is mostly determined by the gas density in a galaxy, while AGN activity is more closely related to the host property such as mass and luminosity that are thought to be dependent on the environment through the density-luminosity relation.

Keywords: barred galaxy, bar strength, star formation rate, AGN

요 약: 본 연구에서는 SDSS DR6을이용하여 별탄생율과 활동성 은하핵의 막대의 특성, 특히 막대의 세기에 대한 의존성을 조사하였다. 막대의 세기를 보다 잘 표현하기 위하여 막대의 길이와 축비를 이용하여 막대를 6개의 군으로 나누었다. Hα 방출선 세기로 부터 구한 별탄생율은 막대의 세기와 좋은 상관관계를 보였으나 활동성 은하핵은 막대와 또렷한 상관관계를 보이지 않았다. 전자의 상관관계는 막대에 의해 유발되는 가스 유입이 막대의 세기에 의존하기 때문이라고 해석되며, 활동성 은하핵이 막대의 특성과 특별한 상관관계를 보이지 않는 것은 초중량 블랙홀로 들어가는 가스의 양이 막대와 초거대 블랙홀과의 상호 작용에 의해 조절된다는 것을 의미한다. 활동성 은하핵은 주변의 밀도에 의해 영향을 받으나 별탄생율은 주변의 밀도와 무관해 보인다. 이것은 별탄생은 은하에서의 가스 밀도에 의해 결정되는 국지적인 현상인데 반해 활동성 은하핵은 질량이나 광도와 같은 은하의 특성이 밀도-광도관계로 표현되는 은하의 환경 의존성과 밀접한 관계가 있음을 암시한다.

주요어: 막대은하, 막대의 세기, 별탄생율, 활동성 은하핵

Introduction

Bar is one of the most common features of galaxies; more than 60% of bright spiral galaxies have bar feature (e.g., Knapen et al., 2000; Eskridge et al., 2002; Barazza et al., 2008; references therein). There are several investigations of bar properties based on the detailed surface photometry (Elmegreen and Elmegreen, 1985; Ann and Lee, 1987; Otha et al., 1990; Martin, 1995; Laurikainen et al., 2002) to understand the structure of barred galaxies.

The nuclear activity of barred galaxies is thought to be correlated with the bar strength (Martinet and

*Corresponding author: hbann@pusan.ac.kr
Tel: 82-51-510-2705
Fax: 82-51-513-7495

Friedli, 1997; Ho et al., 1997) because the non-axisymmetric potential of bars are effective in driving inflow of the disk material toward the center of galaxies (Simkin et al., 1980; Wada and Habe, 1992; Friedli and Benz, 1993, 1995; Ann and Lee, 2000; Regan and Teuben, 2004). However, the correlation between the bar strength and the nuclear activity seems to be not clear since there is little difference in the star formation rates between non-barred galaxies and barred galaxies (Pompea and Rieke, 1990; Isobe and Feigelson, 1992). Moreover, some optical studies argued that there is no relationship between the bar properties and the nuclear activity (Ho et al., 1997, Marquez et al., 2000, Laurikainen et al., 2001).

Since the bar-driven gas inflow toward the nuclear regions is thought to be well understood theoretically (Englmaier and Shlosman, 2000; Maciejwesky et al., 2002; Regan and Teuben, 2004; Ann and Thakur, 2005 and references therein) and supported by observations (e.g., Knapen et al., 2000; Sheth et al., 2005), the observational results that show little or no correlation between the nuclear activty and bar strength (Pompea and Rieke, 1990; Isobe and Feigelson, 1992; Ho et al., 1997; Marquez et al., 2000; Laurikainen et al., 2001) are quite surprising. There seem to be two possibilities for the lack of correlations between the nuclear activity and bar strength. One is the probable anti-correlation between the mass of supermassive black hole (SMBH) and the bar strength because bars are likely to be destroyed by the central mass concentration (Hassen et al., 1993; Norman et al., 1996). Since the nuclear activity of galaxies is supposed to be correlated with the mass of SMBH as well as the gas infall rate driven by the non-axisymmetric potential, little or no correlation between the nuclear activity and bar strength is not unexpected. The other is that the previous observational results (Ho et al., 1997; Marquez et al., 2000) are due to the small sample size that induces a statistical noise to make weak correlations invisible. The latter view is supported by the presence of small difference in the bar properties between non-barred galaxies and barred galaxies when the sample size is significantly increased (Laurikainen et al., 2001; Laurikainen et al., 2002, 2004).

The aim of the present paper is to understand whether there is a correlation between the nuclear activity and bar strength. To do this, we analyze the star formation rate and AGN of barred galaxies using a flux limited sample of barred galaxies obtained from the Sloan Digital Sky Survey (SDSS). For a reasonable measure of the bar strength, we devised a new index to represent the bar strength using the deprojected length and axial ratio of a bar where the bar length is in unit of the optical diameter of the bar.

The organization of the present paper is as follows. In the next section, we describe the basic observational data and measurement of bar lengths along with the derivation of the bar strength. We describe how to determine the star formation rate and AGN in section 3 and the correlations between the nuclear activities and bar properties in section 4. We discuss the bar-driven star formation and AGN in section 5, and conclusions are given in the final section.

Observational Data and Bar Properties

Sample

The basic data of the present study is the SDSS Data Release 6 (DR6). We selected 465 barred galaxies from the primary sample of 5451 galaxies that are in the redshift range $0.01<z<0.02$ by visual classification using color images provided by SDSS archive. Since spectroscopic observations are confined to the galaxies with Petrosian r-band magnitude of $14.5<r<17.7$, our sample of galaxies are brighter than $Mr\approx-15.5$ and most of the primary sample of galaxies are large enough for visual classification. We excluded some barred galaxies that are too small to measure the axis lengths of bars or have bars with transition shape.

In Fig. 1 we present four examples of typical barred galaxies from the primary sample of galaxies. Fig. 1a shows the example of the clearest bar, whereas Fig. 1d shows that of the most unclear bar. The bars

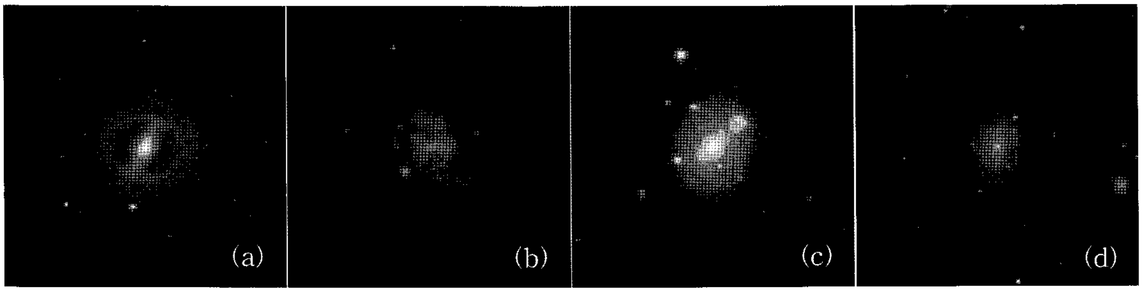

Fig. 1. Example of color images of barred galaxies. The bar shape is well identified in (a)-(c). The galaxy in (d) is an example of galaxies that show a transition type (SAB) morphology. We excluded galaxies that show a morphology similar to (d) in the present analysis.

similar to those in Fig. 1a-1c are clear enough to measure the bar axis lengths, but the bars resembling that in Fig. 1d are difficult to measure the bar axis lengths properly. Thus, we confine our final sample of barred galaxies to those have bars more clear than that shown in Fig. 1d.

Length and axial ratio of bars

Length of bars: The length of a bar is a directly measurable quantity using photographic plates or CCD images. We measured the length of bars from the color images provided by SDSS archive using SAO (Smithsonian Astrophysical Observatory) image display tool. Because the measured length of a bar is not the true length due to the inclination of the disk to the line of sight, we deprojected the measured bar length to determine the true length of a bar using the formulae used by Martin (1995),

$$l_B=2a(\cos^2\phi_a+\sec^2 i\sin^2\phi_a)^{1/2}$$

where a is the semi-major axis of the bar, i is the inclination angle of the galaxy, and ϕ_a is the angle between the bar major axis and the line of node. We derived the true length of a bar in kiloparsecs using the co-moving distance of galaxies from NED (NASA/IPAC Extragalactic Database) which assumes ΛCDM cosmology that adopted with H=73 km/s/Mpc, Ω_Λ=0.73, Ω_m=0.27. We also calculated the relative bar length scaled to the optical diameter of the galaxy $L_b(i)$. We used the r-band Petrosian radius as the representative optical radius of a galaxy. The inclination angle i is calculated from the semi-major and semi-minor axes of the bar measured in the present study.

Axial ratios: We obtained the axial ratio of bars from the major and minor axis lengths measured from the color images of SDSS DR6. Visual measurement of bar axis length has some uncertainties inherent in the eyeball estimation. However the most significant source of errors is contamination of bulge luminosity. It is more serious in measuring the minor axis length of bar. We followed the method of Martin (1995) to estimate the bar semi-major axis, i.e., we defined the semi-major axis as the length from the galaxy center to the sharp outer tip of the bar-shaped component. For the minor axis of a bar, we measured the length of minor axis at the middle of the semi-major axis rather than at the center of a galaxy to reduce the effect of bulge contamination.

Since we excluded the galaxies with unclear bar shape, the semi-major axis length of a bar measured at the middle of the bar semi-major axis is not much different from the true length of the semi-minor axis of a bar. To determine the inclination-corrected bar axial ratio, we applied the method of Martin (1995) as follows,

$$\frac{b}{a}(i)=\frac{b}{a}\left[\frac{\cos^2\phi_b+\sec^2 i\sin^2\phi_b}{\cos^2\phi_a+\sec^2 i\sin^2\phi_a}\right]^{1/2}$$

where a and b are semi-major and semi-minor axis length, respectively, i is the inclination angle of the galaxy, ϕ_a and ϕ_b are the angles between the bar axes and the line of nodes.

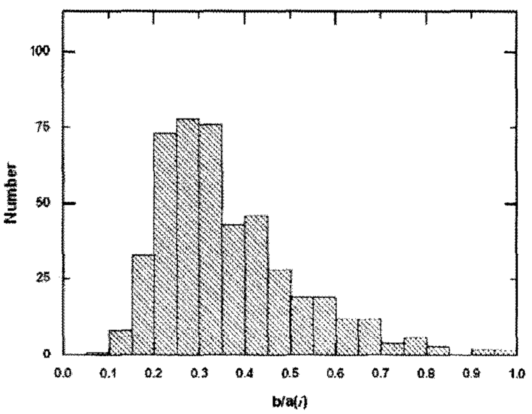

Fig. 2. The distribution of bar axial ratio b/a(*i*) of the sample of galaxies.

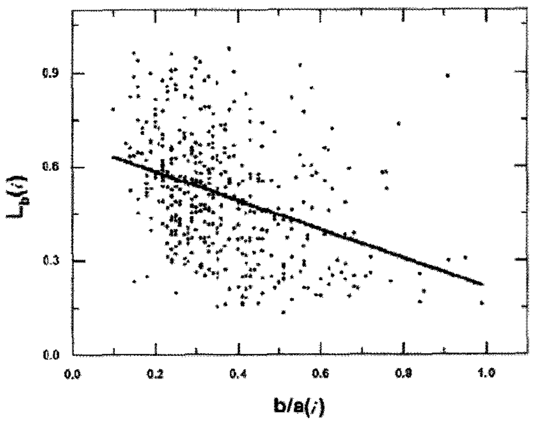

Fig. 3. The bar axial ratio b/a(*i*) versus the relative bar length $L_b(i)$. The dotted line divides strong bars and weak bars and the thin solid line divides long bars and short bars.

In Fig. 2, we presented the distribution of the deprojected axial ratio of bar, b/a(*i*), which shows that the bars in the present sample are in general more elongated than those of the previous studies (Martin, 1995; Martinet and Friedli, 1997). There are two reasons for this tendency; the different definition of the length of semi-minor axis, and the selection criteria of our sample of galaxies. Since our estimates of the length of bar semi-minor axis are systematically smaller than others, especially for early type barred galaxies with large bulges which make the semi-minor axis of bar longer than the actual one, the smaller $\frac{b}{a}(i)$ from our estimates is expected. The exclusion of the galaxies with transition morphology (SAB) also contributes to the excess of the elongated bars in our sample.

Bar strength: It is not easy to estimate the bar strength from observations even though there is no difficulty to define the bar strength theoretically. The widely used definition of the bar strength is the maximal tangential force in terms of the mean radial force, Q_b (Combes and Sanders, 1981). However, the calculation of bar strength using this definition requires a complicated procedure including the derivation of the galaxy potential from a deep surface photometry. Owing to the practical difficulty to determine Q_b from surface photometry, the length and axial ratio of bars are frequently used to represent the bar strength. However, as noted by a recent investigation of Laurikainen et al. (2002), the length of a bar is not a good indicator of bar strength.

The bar axial ratio seems to be correlated with the bar strength by theoretical ground (Athanassoula, 1992) as well as by observation (Laurikainen et al., 2002). However, as shown in Fig. 3, there is a moderate correlation with a correlation coefficient of −0.37 between the deprojected bar axis ratio b/a(*i*) and bar length relative to the optical diameter derived from the *r*-band Petrosian radius. Although the linear least-squares fit seems to be not adequate to represent the correlation between the bar axis ratio and bar length, it does show a tendency of more elongated shape for larger bars.

However, the bar strength defined above, is correlated with not only the bar axial ratio but also the luminosity of a bar. Bars having a small axial ratio and a large luminosity are strong, whereas bars having a large axial ratio and small luminosity are weak. Thus it seems better to use both parameters together to represent the strength of a bar. We divided bars into 6 classes by introducing a strength index, S_b, which are defined by the combined criteria for the length and axial ratio of bars. To do this, we divided bars into two length groups, <7 kpc and >7 kpc and three axial ratio groups, $b/a(i)<0.25$, $0.25<b/a(i)$ 0.55, and $b/a(i)>0.55$. The weakest bar, $S_b=1$, has a bar length

Table 1. Bar strength classes with the length and axial ratio of bars

S_b	1	2	3	4	5	6
b/a(*i*)	>0.55	0.25-0.55	≤0.25	>0.55	0.25-0.55	≤0.25
a(*i*) (kpc)	≤7	≤7	≤7	>7	>7	>7
Number	44	186	43	16	104	72

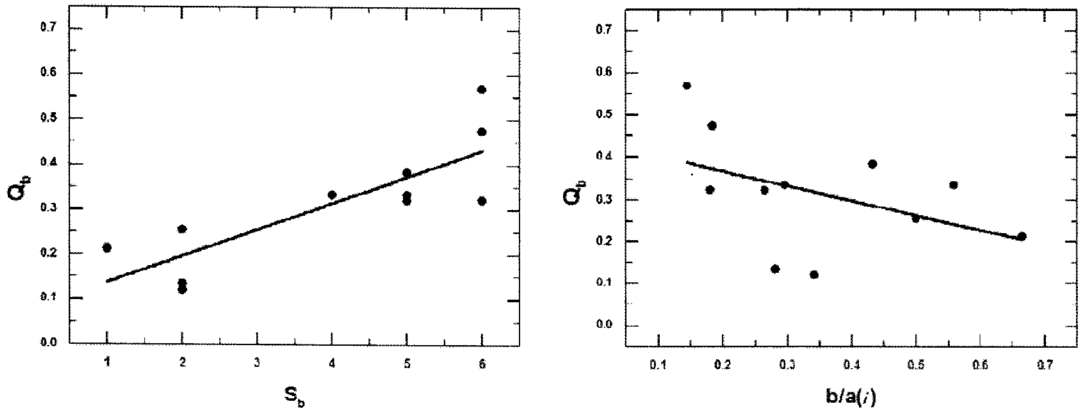

Fig. 4. Comparisons of the true bar strength Q_b and strength index S_b(left) and bar axis ratio b/a(*i*) (right) for 11 galaxies common between this study and Buta et al. (2005). S_b seems to be a better indicator of bar strength than b/a(*i*).

less than 7kpc and an axial ratio greater than 0.55, while the strongest bar, S_b=6, has a bar length greater than 7 kpc and an axial ratio less than 0.25. The bar length of 7 kpc is the mean length of bars for the galaxies in the present sample. We listed S_b class and their criteria in Table 1. Fig. 4 shows a comparison between S_b and Q_b that shows the usefulness of the strength index introduced above. We used the Q_b values reported by Buta et al. (2005) who calculated Q_b for 147 bright galaxies from *H*-band surface photometry of which we found 12 galaxies common in the present sample (Table 2). As shown in Fig. 4, there is a good correlation between the strength index S_b and true bar strength Q_b, whereas the axial ratio of bar shows a less tight correlation with Q_b.

Star formation rate and AGN

We have used the emission lines of the present sample provided by SDSS DR6. We summarized the statistics of the emission lines in Table 3. Among the emission lines listed in Table 3. lines are the strongest ones of which 55% have equivalent width (EW) larger than three times the measurement error, i.e, signal to noise ratio (S/N)>3, while only 25% of lines and 13% of [OIII] lines have S/N>3. It is better to use emission line data with S/N>3 for the analysis of nuclear activity. However, we used all the galaxies that have emission lines with S/N>1 for better statistics.

Table 2. Bar properties and true bar strength for 11 galaxies common between this study and Buta et al. (2005)

Galaxy	a(")	b(")	a/b(*i*)	S_b	Q_b
NGC 6385	12.0	3.4	0.28	2	0.135
NGC 5335	20.3	4.0	0.18	6	0.322
NGC 0151	17.9	5.8	0.18	6	0.475
NGC 0291	4.3	1.5	0.66	1	0.212
NGC 3895	11.4	2.9	0.34	2	0.122
NGC 4025	18.5	2.6	0.14	6	0.569
NGC 2558	10.4	4.4	0.56	4	0.334
NGC 2557	12.8	3.3	0.30	5	0.334
NGC 5641	20.6	2.9	0.27	5	0.321
NGC 5430	22.7	7.7	0.43	5	0.383
NGC 5923	6.1	2.8	0.50	2	0.255

Star formation rate: There are several indicators of recent star formation such as the $H\alpha$ luminosity (Ho et al., 1997; Kennicutt, 1998), the far-infrared (FIR)

Table 3. Statistics of the emission line strength (strong: signal to noise ratio (S/N)>3, weak: S/N>1)

	Hα			Hβ		
	strong	weak	no	strong	weak	no
Number	258	44	163	115	107	243
Percentage(%)	55	9	35	25	23	52
	[OIII] λ5007			[NII] λ6583		
	strong	weak	no	strong	weak	no
Number	60	79	326	157	151	157
Percentage(%)	13	17	70	34	32	34

emission ratio of I_{25}/I_{100} where I_{25} and are I_{100} the IRAS fluxes at 25 μm and 100 μm (Martinet and Friedli, 1997; Aguerri, 1999), the $H\delta_A$ index (Kauffmann et al., 2003), and the UV emission (Donas et al., 1987). But, We used the Hopkins et al. (2001)'s method to calculate the star formation rate because it corrects the obscuration and aperture effect reliably using the SDSS emission lines. Hopkins et al. (2003) used Hα and Hβ emission lines and r-band magnitude of galaxies to calculate,

$$SFR_{H\alpha}(M_{\odot}yr^{-1}) =$$
$$4\pi D_l^2 S_{H\alpha} 10^{-0.4(r_p - r_f)} \left(\frac{S_{H\alpha}/S_{H\beta}}{2.86}\right)^{2.114} \frac{1}{1.27\times10^{34}}$$

where D is the co-moving radial distance, r_p and r_f and are r-band petrosian magnitude and fiber magnitude, respectively, and $S_{H\alpha}$ and $S_{H\beta}$ are the stellar absorption-corrected H_α and H_β line flux, respectively, defined by

$$S_{H\alpha} = \frac{EW+EW_c}{EW}F, \quad S_{H\beta} = \frac{EW+EW_c}{EW}F$$

where EW is equivalent width of the line, EW_c is the correction for stellar absorption (commonly EW_c= 2Å), and F is the observed line flux. Star formation rate which calculated from the above method is well-correlated with other indicators such as FIR and 1.4 GHz luminosity (Hopkins et al., 2003). In the following, star formation rate is assumed to be high if $\log(SFR_{H\alpha})\geq 0$, and low if $\log(SFR_{H\alpha})<0$, following Hopkins et al. (2003).

AGNs: Since Veilleux and Osterbrock (1987) proposed a diagnostic tool for AGN classification using four line ratios; [OIII] λ5007/Hβ, [NII] λ6583/Hα, [SII] (λ6716+λ6731)/Hα, and [OI] λ6300/Hα, based on the suggestion of Baldwin et al. (1981), most of the previous studies for AGN classification used similar diagnostics to classify emission-line galaxies into narrow-line AGN and HII region galaxies (e.g., Kewley et al., 2001; Hyung et al., 2006). Kewley et al. (2001) developed a simple rectangular hyperbolic-shaped criterion for these lines to separate AGNs and star-forming galaxies on the diagnostic diagrams. Kauffmann et al. (2003) presented another method, very similar to that of Kewley et al. (2001) but more stringent upper limit for starburst galaxies. They used only two line ratios; [OIII] λ5007/Hβ, and [NII] λ6583/Hα.

Since Kewely et al. (2003)'s criteria do not include weak AGNs, we used the Kauffmann et al. (2003)'s method to identify AGN, i.e., a galaxy is considered to be an AGN if

$$\log([OIII]/H_\beta) > \frac{0.61}{\log([NII]/H_\alpha) - 0.05} + 1.3.$$

We used the [OIII] λ5007, [NII] λ6583, Hα, Hβ emission lines from the spectroscopic data in SDSS DR6.

Correlations Among Derived Properties

Star Formation Rate and Bar Strength

The interplay between the star formation rate derived from H_α emission lines $SFR_{H\alpha}$ and bar

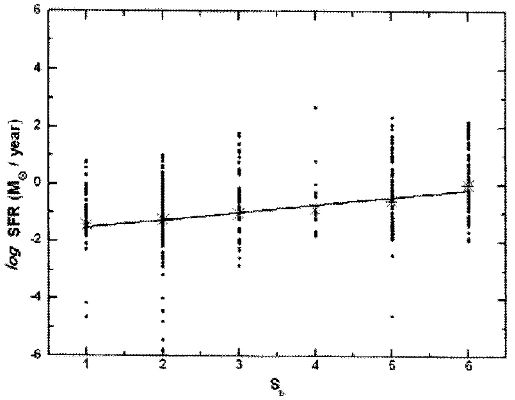

Fig. 5. Star formation rate versus bar strength S_b. Star symbols indicate the average values of star formation rate, and the line is the least-square fit.

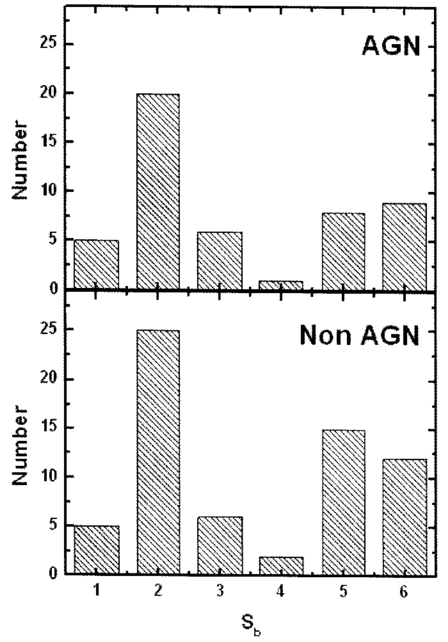

Fig. 6. The frequency distributions of bar strength S_b for AGNs (top) and non-AGNs (bottom).

strength is presented in Fig. 5. As shown by the soild line which represents a least-square fit to the data, there is a tendency of increasing star formation rate with increasing with a large scatter. It means that strongly barred galaxies are likely to induce more star formation than weakly barred galaxies but the scatter is considerable. About 85% of galaxies with $S_b \leq 2$ have $\log(SFR_{H\alpha})<0$, whereas less than half of galaxies with $S_b \geq 5$ show $\log(SFR_{H\alpha}) \geq 0$. This means that the

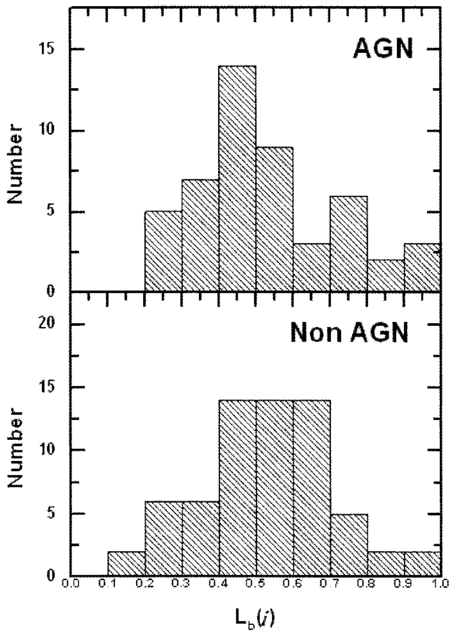

Fig. 7. The frequency distributions of bar length L_b(i) for AGNs (top) and non-AGNs (bottom).

majority of galaxies in the present sample shows low star formation rate ($\log(SFR_{H\alpha})<0$). Although the non star forming strongly barred galaxies seem to be out of the main tendency, they are thought to be in a pre-starburst or in a post-starburst phase (Martinet and Friedli, 1997).

AGN and Bar Properties

It has been not clear whether AGNs are more frequent in barred galaxies than non-barred galaxies. Because the present sample is consists of well defined barred galaxies, it is promising to see whether there is a dependence of frequency of AGN on the bar strength. Since the Kauffmann's method of AGN classification requires four emission lines, [OIII] λ5007, [NII] λ6583, Hα, Hβ, we selected 114 galaxies that have measurable emission for these lines, i.e., EW>σ. We identified 49 AGNs among 114 galaxies. That means ~43.0% of emission line galaxies show AGN characteristics.

Fig. 8 displays the frequency distribution of the bar strength index S_b for AGN and non-AGN galaxies. As shown in Fig. 8, there is no significant difference

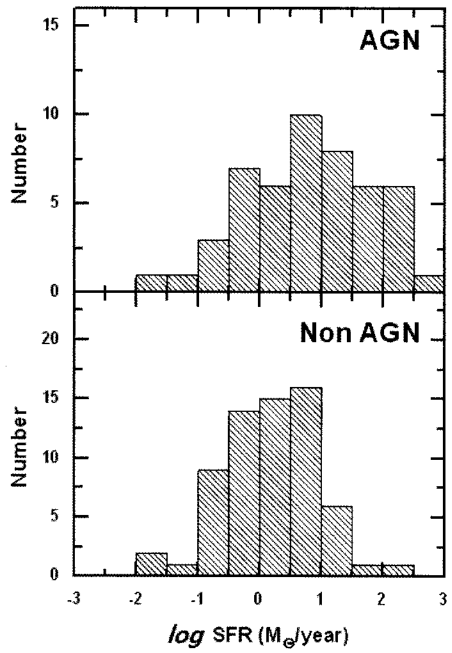

Fig. 8. The frequency distributions of nuclear star formation rates for AGNs (top) and non-AGNs (bottom).

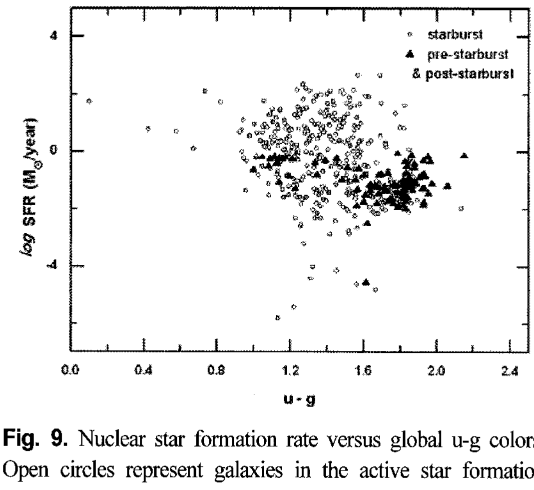

Fig. 9. Nuclear star formation rate versus global u-g colors. Open circles represent galaxies in the active star formation phase and the filled triangles indicate the galaxies in the pre-starburst phase and post-starburst phase.

between the AGN and non-AGN galaxies. It means that there is no dependence of AGN activity on the bar strength. The frequency distributions of the bar lengths scaled to the optical diameter of a galaxy shows a similar result (Fig. 9). Thus, it can be concluded that the bar properties are not directly related to the presence of AGNs even though bars can

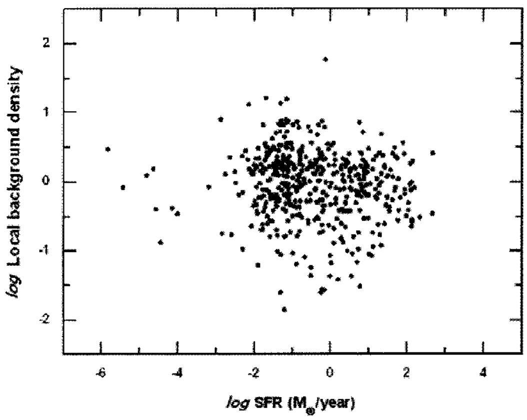

Fig. 10. Nuclear star formation rate versus local background density.

provide the fuels of AGN by driving gas inflow toward the galactic nuclei. We will discuss the causes for the lack of corelation between the bar strength and AGN activity in the next section.

AGN and Star Formation Rate

Fig. 10 shows the frequency distribution of star formation rate for AGN and non-AGN galaxies. There is a significant difference between the two populations. The average star formation rate of galaxies that host AGN (0.78 $M_{\odot}/yr$) is more than three times larger than those of non-AGN galaxies (0.19 $M_{\odot}/yr$). In terms of Hopkins et al. (2003)'s criteria for high and low star formation rate, 42% of non-AGN galaxies has low star formation rate, while only 24% of AGN galaxies has low star formation rate.

It is quite interesting that star formation rate correlates with bar strength as well as AGN, while there seems to be no apparent correlation between AGN and bar strength. It suggests that star formation is simply related to the gas supply which is controlled by the bar strength. But, the presence of AGN requires other condition that is closely related to the characteristics of emission lines. It seems to be the mass of SMBH since mass accretion to the SMBH is thought to be modulated by its mass (Son and Hyung, 2004). Bars can transport disk gas to the nuclear regions but there are some barriers caused by the orbital resonances between the non-axisymmetric

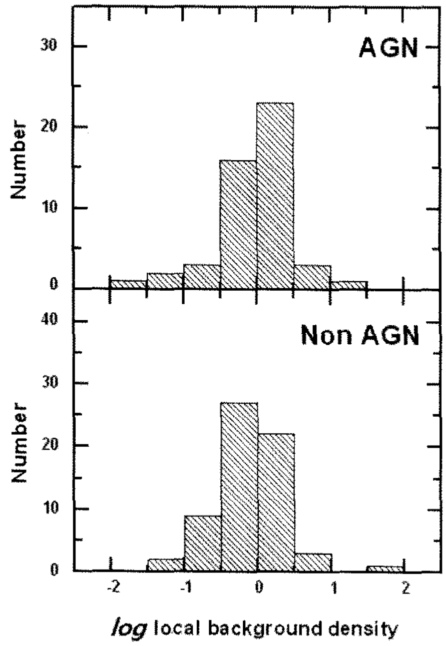

Fig. 11. The frequency distributions of local background density for AGNs (top) and non-AGNs (bottom).

potential and axisymmetric potentials (Englmaier and Shlosman, 2000).

Among nuclear features, the nuclear ring at Inner Lindblad Resonance (ILR) is thought to prevent the gas infall to the nucleus (Piner et al., 1995; Ann and Lee, 2000; Reagan and Teuben, 2004). Because the strength of ILR depends on the central mass concentration, centrally concentrated galaxies that are thought to have a large SMBH are likely to have nuclear rings. However, when sound speed of gas is high enough, gas can penetrate the barrier imposed at ILR and spiral in all the way to the nucleus (Maciejewski et al., 2002; Ann and Thakur, 2005). Thus, violent environment that might be related to the presence of a large SMBH may help gas infall that can be fuels of AGN as well as massive star formation.

Discussion

Bar-driven Star Formation

It appears that there is a close connection between the bar strength and the star formation activity. Strong bars are likely to enhance the star formation rate than weak bars. Aguerri (1999) showed a similar result for isolated barred galaxies. The dependence of star formation rate on the bar strength is explained by the role of bars in the secular evolution where bar drives disk gas toward the center of galaxies by hydrodynamic processes (Friedli and Bens, 1993, 1995; Ann, 2003). However, the fact that more than a half of the galaxies that have strong bars show low star formation rate requires some mechanism which regulates the bar driven star formation.

Martinet and Friedli (1997) showed that in a secular evolution scenario, a weakly barred galaxy has low star formation rate in the early stage of evolution but it evolves to a galaxy with a moderately strong bar without active star formation at the nucleus. This stage of evolution is pre-starburst phase. When the bar becomes strong enough, the inflow of gas toward the center of a galaxy is increased and the star formation rate is increased as well. If the gas is exhausted at the nucleus with no more gas inflow due to lack of gas in the disk, the star formation is diminished although the bar remains as strong (post-starburst phase). This is the reason why we observe low star formation rates in strongly barred galaxies.

The global *u-g* color index of galaxies in a pre-starburst phase and a post-starburst phase is shown in Fig. 13. In general, the colors of these galaxies are redder than other galaxies due to lack of gas in the disk, which means no more star formation in the disk. Thus, the non-star forming, strongly barred galaxies are thought be in a pre-starburst or in a post-starburst phase. The decreasing bar fraction with the redshift found from the Cosmic Evolution Survey (Scoville et al., 2007) is consistent with the scenario that strong bars with low star formation rates are in a post-starburst phase due to a secular evolution, since strong bars are basically the result of an early dynamical evolution which accompanies the mass assembly (Sheth et al., 2008).

Interplay between bars and AGN

The ratio of AGN in our sample is greater than the ratio of AGN in galaxies at 0.02<z<0.3; 43% in our sample and 18% in Kauffmann et al. (2003). Since our sample includes barred galaxies only while Kauffmann et al. (2003)'s sample includes all the galaxies in the redshift ranges, we can assume that the presence of a bar provides a favorable condition for AGN. However, as shown in Fig. 8, the presence of AGN is not related to the bar strength. Since strong bars drive more gas inflow than weak bars, it seems that the presence of gas in the nuclear region is not a sufficient condition for AGN. To activate AGN, a sufficient amount of gas should be continuously accreted to the nucleus. But, the bar-induced accretion is episodic and insufficient (Ho et al., 1997). Moreover, the gas inflow toward nucleus through the ILRs are strongly affected by the mass of SMBH as well as the sound speed of gas (Ann and Lee, 2004; Ann and Thakur, 2005). Because of these reasons, the bar strength can not be directly related to the presence of AGN.

Environment dependence

It is well known that formation and evolution of galaxies depends much on the environment of the galaxy: the density-morphology relation (Dressler, 1980) and density-luminosity relation (Park et al., 2007). As shown in Fig. 10, there is no correlation between the star formation rate and the local background density representing the logarithm of normalized background density $\log\rho/\rho_m$ where ρ_m is the mean background density. We adopted the method of van der Wel et al. (2008) to calculate the background density (ρ) which is defined by the number of galaxies divided by the projected area enclosed by a radius R. R is the distance to the 7th nearest L* galaxies whose mass is greater than $4\cdot10^{10}$ $M_{\odot}$. The lack of correlation revealed in Fig. 10 suggests that the local background density is not much relevant to the star formation rate. Since the star formation is closely related to the amount of gas in the nuclear regions of a diameter less than 1 kpc while local background density represent a mean environment over a few Mpc, the irrelevance of the nuclear star formation rate with the local background density seems to be understandable.

However, there seems to be a weak dependence of AGN activity on the local background density, as shown in Fig. 11. The mean local density of galaxies that host AGN is about five times larger than that of the non-AGN galaxies. The reason for the apparent preponderance of AGNs in the high density environment is the dependence of galaxy luminosity on the local background density through density-luminosity relation. Since the mass of SMBH is proportional to the bulge mass, it is quite plausible that galaxies with AGN are likely to have large bulges which are preferentially found in the high density regions (Park et al., 2007).

Conclusions

We analyzed the dependence of star formation rate and AGN frequency on the bar properties, in particular the bar strength. We measured the bar properties such as bar lengths and axial ratios visually, using color images from the SDSS DR6. We devised a new indicator of bar strength Sb by combining the length and axial ratio of bar, which is found to be well correlated with the true bar strength (Q_b) derived from the potential distributions. Our results can be summarized as follows:

i) Strongly barred galaxies are likely to have higher star formation rate ($\log(SFR_{H\alpha})\geq0$) than weakly barred galaxies, The reason for this correlation is thought to be the bar-driven gas inflow which supplies a plenty of gas for star formation. However, the majority of galaxies in the present sample show low star formation rates, implying less gas in the disk than non-barred galaxies due to a fast dynamical evolution in massive galaxies.

ii) There seems to be no apparent correlation between the occurrence of AGN and the bar properties such as bar axial ratios and the bar lengths scaled to the optical diameter of a galaxy as well as the bar strength derived in the present study. It implies that the presence of gas in the nuclear regions due to the bar-driven gas inflow is not sufficient to activate AGN. Since the gas accretion onto the SMBH is regulated by many factors such as the gas sound speed, mass of SMBH, and bar strength. all of which are closely related, the lack of correlation between AGN and bar strength is not unexpected.

iii) There is no correlation between the star formation rate and the local background density, whereas there is a clear dependence of the freuency of AGNs on the local background density. It suggests that star formation is a localized phenomenon which is directly related to the gas density in a galaxy while AGN is more closely related to the integral property of a galaxy such as mass of host galaxies that is affected by the environment through density-luminosity relation.

Acknowledgments

This work was supported for two years by Pusan National University Research Grant.

References

Aguerri, J.A.L., 1999, A strong correlation between bar strength and Global Star Forming Activity in Isolated Barred Galaxies. Astronomy and Astrophysics, 351, 43-46.

Ann, H.B. 2003, Secular Evolution of Barred Galaxies. Journal of the Korean Astronomical Society, 36, 241-248.

Ann, H.B. and Lee, S.-W. 1987, Surface Photometry of Barred Galaxies: Global Structure of Barred Galaxies. Journal of the Korean Astronomical Society, 20, 49-62.

Ann, H.B. and Lee, H.M. 2000, SPH Simulations of Barred Galaxies: Dynamical Evolution of Gaseous Disk. Journal of the Korean Astronomical Society, 33, 1-17.

Ann, H.B. and Lee, H.M. 2004, Nuclear Spirals as Signatures of Supermassive Black Holes. The Astrophysical Journal, 613, L105-L108.

Ann, H.B. and Thakur, 2005, Formation of Nuclear Spirals in Barred Galaxies. The Astrophysical Journal, 620, 197-209.

Athanassoula, E., 1992, The Existence and Shapes of Dust Lanes in Galactic Bars. Monthly Notices of the Royal Astronomical Society, 259, 345-364.

Baldwin, J., Phillips, M., and Terlevich, R., 1981, Classification Parameters for the Emission-line Spectra of Extragalactic Objects. Publications of the Astronomical Society of the Pacific, 93, 5-19.

Barazza, F.D., Jogee, A., and Marinova, I., 2008, Bars in Disk-dominated and Bulge-dominated Galaxies at z ~ 0: New Insights from ~3600 SDSS Galaxies. The Astrophysical Journal., 675, 1194-1212.

Buta. R., Vasylyev, S., Salo, H., and Laurikainen, E. 2005, The Distribution of Bar and Spiral Arm Strengths in Disk Galaxies. The Astronomical Journal, 130, 506-523.

Combes, F. and Sanders, R.H., 1981, Formation and Properties of Persisting Stellar Bars. Astronomy and Astrophysics, 96, 164-173.

Donas, J., Deharveng, J.M., Milliard, B., Laget, M., and Huguenin, D., 1987, Ultraviolet Observations and Star-formation Rate in Galaxies. Astronomy and Astrophysics, 180, 12-26.

Dressler, A., 1980, Galaxy Morphology in Rich Clusters - Implications for the Formation and Evolution of Galaxies. The Astrophysical Journal, 236, 351-365.

Elmegreen, B.G. and Elmegreen, D.M., 1985, Properties of Barred Spiral Galaxies. The Astrophysical Journal, 288, 438-455.

Englmaier, P. and Shlosman, I., 2000, Density Waves inside the Inner Lindblad Resonance: Nuclear Spirals in Disk Galaxies. The Astrophysical Journal, 528, 677-686.

Eskridge, P.B., Frogel, J.A., Pogge, R.W., Quillen, A.C., Berlind, A.A., Davies, R.L., DePoy, D.L., Gilbert, K.M., Houdashelt, M.L., Kuchinski, L.E., Ramirez, S.V., Sellgren, K., Stutz, A., Terndrup, D.M., and Tiede, G.P., 2002, Near-Infrared and Optical Morphology of Spiral Galaxies. The Astrophysical Journals, 143, 73-111.

Friedli, D. and Benz, W., 1993, Secular Evolution of Isolated Barred Galaxies. I-Gravitational Coupling between Stellar Bars and Interstellar Medium. Astronomy and Astrophysics, 268, 65-85.

Friedli, D. and Benz, W., 1995, Secular Evolution of Isolated Barred Galaxies. II. Coupling between Stars and Interstellar Medium via Star Formation. Astronomy and Astrophysics, 301, 649-665.

Hasan, H., Pfenniger, D., and Norman, C., 1993, Galactic Bars with Central Mass Concentrations-Three-dimensional Dynamics. The Astrophysical Journal, 409, 91-109.

Ho, L.C., Filippenko, A.V., and Sargent, W.L.W., 1997, The Influence of Bars on Nuclear Activity. The Astrophysical Journal, 487, 591-602.

Hopkins, A.M., Miller, C.J., Nichol, R.C., Connolly, A.J. et al., 2003, Star Formation Rate Indicators In The Sloan Digital Sky Survey. The Astrophysical Journal, 599, 971-991.

Hyung, S., Son, D.-H., Ferruit, P., and Lee, W.-B. 2006, OASIS Spectral Images of the Seyfert galaxy NGC

5728. Journal of Korean Earth Science Society, 27, 569-578.

Isobe, T. and Feigelson, E.D. 1992, Far-infrared Luminosity Functions of Normal Galaxies. The Astrophysical Journal, 79, 197-211.

Kauffmann, G., Heckman, T.M., Tremonti, C., Brinchmann, J., Charlot, S., White, S.D.M., Ridgway, S.E., Brinkmann, J., Fukugita, M., Hall, P.B., Ivezi, Z., Richards, G.T., and Schneider, D.P., 2003, The Host Galaxies of Active Galactic Nuclei. Monthly Notices of the Royal Astronomical Society, 346, 1055-1077.

Kennicutt, R.C.Jr., 1998, Star Formation in Galaxies Along the Hubble Sequence. Annual Review of Astronomy and Astrophysics, 36, 189-231.

Kewley, L.J., Dopita, M.A., Sutherland, R.S., Heisler, C.A., and Trevena, J., 2001, Theoretical Modeling of Starburst Galaxies. The Astrophysical Journal, 556, 121-140.

Knapen, J.H., Shlosman, I., and Peletier, R., 2000, A Subarcsecond Resolution Near-Infrared Study of Seyfert and Normal Galaxies. II. Morphology. The Astrophysical Journal, 529, 93-100.

Laurikainen, E., Salo, H., and Rautiainen, P., 2001, Bar Strengths and Nuclear Activity. Astronomical Society of Pacific Conference Series, 249, 183-186.

Laurikainen, E., Salo, H., and Rautiainen, P., 2002, Comparison of Bar Strengths in Active and Non-active Galaxies. Monthly Notices of the Royal Astronomical Society, 331, 880-892.

Laurikainen, E. and Salo, H., 2004, Comparison of Bar Strengths and Fractions of Bars in Active and Nonactive Galaxies. The Astrophysical Journal, 607, 103-124.

Maciejewski, W., Teuben, P.J., Sparke, L.S., and Stone, J.M., 2002, Gas Inflow in Barred Galaxies - Effects of Secondary Bars. Monthly Notices of the Royal Astronomical Society, 329, 502-512.

Márquez, I., Durret, F., Masegosa, J., Moles, M., Gonzalez Delgado, R.M., Marrero, I., Maza, J., Perez, E., and Roth, M., 2000, Near-infrared Photometry of Isolated Spirals with and without an AGN-II. Photometric Properties of the Host Galaxies. Astronomy and Astrophysics, 360, 431-438.

Martin, P., 1995, Quantitative Morphology of Bars in Spiral Galaxies. The Astronomical Journal, 109, 2428-2443.

Martinet, L. and Friedli, D. 1997, Bar Strength and Star Formation Activity in Late-type Barred Galaxies. Astronomy and Astrophysics, 323, 363-373.

Norman, C.A., Sellwood, J.A., and Hasan, H. 1996, Bar Dissolution and Bulge Formation: An Example of Secular Dynamical Evolution in Galaxies. The Astrophysical Journal, 462, 114-124.

Ohta, K., Hamabe, M., and Wakamatsu, K., 1990, Surface Photometry of Barred Spiral Galaxies. The Astrophysical Journal, 357, 71-90.

Park, C., Choi, Y.-Y., Vogeley, M.S., Gott, J.R., and Blanton, M.R., 2007, Environmental Dependence of Properties of Galaxies in the Sloan Digital Sky Survey. The Astrophysical Journal, 658, 898-916.

Piner, B.G., Stone, J.M., and Teuben, P.J., 1995, Nuclear Rings and Mass Inflow in Hydrodynamic Simulations of Barred Galaxies. The Astrophysical Journal, 449, 508-520.

Pompea, S.M. and Rieke, G.H., 1990, A Test of the Association of Infrared Activity with Bars. The Astrophysical Journal, 356, 416-429.

Regan, M.W. and Teuben, P.J., 2004, Bar-driven Mass Inflow: How Bar Characteristics Affect the Inflow. The Astrophysical Journal, 600, 595-612.

Scoville, N., Abraham, R.G., Aussel, H., Barnes, J.E. et al., 2007, COSMOS: Hubble Space Telescope Observations The Astrophysical Journal Supplement Series, 172, 38-45.

Sheth, K., Vogel, S.N., Regan, M.W., Thornley, M., and Teuben, P.J., 2005, Secular Evolution via Bar-driven gas Inflow: Results from BIMA SONG. The Astrophysical Journal, 632, 217-226.

Sheth, K., Elmegreen, D.M., Elmegreen, B.G., Capak, P. et al., 2008, Evolution of the Bar Fraction in COSMOS: Quantifying the Assembly of the Hubble Sequence. The Astrophysical Journal, 675, 1141-1155.

Simkin, S.M., Su, H.J., and Schwarz, M.P., 1980, Nearby Seyfert Galaxies. The Astrophysical Journal, 237, 404-413.

Son, D.-H. and Hyung, S., 2004, BLR Density Variations of the Seyfert 1 Galaxies NGC 4151 and NGC 5548. Journal of Korean Earth Science Society, 25, 495-501.

van den Wel, A., 2008, The Dependence of Galaxy Morphology and Structure on Environment and Stellar Mass. The Astrophysical Journal, 675, L13-L16.

Veilleux, S. and Osterbrock, D.E., 1987, Spectral Classification of Emission-line Galaxies. The Astrophysical Journal Supplement Series, 63, 295-310.

Wada, K. and Habe, A., 1992, Rapid Gas Supply to a Nuclear Region by Self-gravitational Instability in a Weak Barred Potential. Monthly Notices of the Royal Astronomical Society, 258, 82-94.

2008년 12월 19일 접수
2009년 1월 23일 수정원고 접수
2009년 1월 30일 채택